On Scalable Multiobjective Test Problems With Hardly Dominated Boundaries

Zhenkun Wang, Yew-Soon Ong, *Fellow, IEEE*, and Hisao Ishibuchi, *Fellow, IEEE*

***Abstract*—The DTLZ1–DTLZ4 problems are by far one of the most commonly used test problems in the validation and comparison of multiobjective optimization evolutionary algorithms (MOEAs). However, very recently, it has been pointed out that they have the following two special characteristics: 1) the regularly oriented Pareto front shape and 2) the single distance function. As a modification of them, this paper presents a new set of test problems mDTLZ1–mDTLZ4 to avoid the two special characteristics. Using these new test problems, we investigate the performance of three representative multiobjective evolutionary algorithms NSGA-II, MOEA/D-Tch, and SMS-EMOA. Experimental results indicate that the performance of NSGA-II and MOEA/D-Tch deteriorates on mDTLZ1–mDTLZ4. Subsequently, our analysis reveals that there exist the hardly dominated boundaries in each of mDTLZ1–mDTLZ4, which hinder the approximation of Pareto dominance-based algorithms and Tchebycheff-decomposition-based algorithms. Furthermore, we summarize that the hardly dominated boundary should be an often encountered problem feature in multiobjective optimization. Last but not least, we point out and validate some coping strategies for dominance-based algorithms and decomposition-based algorithms to overcome the challenges caused by the hardly dominated boundary.**

***Index Terms*—ϵ-dominance, evolutionary algorithm, generalized decomposition, hardly dominated boundaries, multiobjective optimization, test problems.**

I. Introduction

A large number of multiobjective optimization evolutionary algorithms (MOEAs) have been developed for various optimization tasks [1]–[4]. The validation and comparison of them are usually carried out by using a chosen set of benchmarks or test problems [5]. Ideally, the test problems used should be well-understood and feature-rich so that the strengths and weaknesses of each algorithm can be comprehensively identified [6]. Toward such a goal, on the one hand, new test problems with different features need to be continuously designed; on the other hand, the features of the existing test problems require to be thoroughly analyzed and summarized [7].

Recently, several test suites with new features have been presented along with some unprecedented findings on the search behaviors of MOEAs [8]–[14]. For example, Liu *et al.* [15] suggested a set of imbalanced test problems for the investigation of MOEAs. And they found that MOEAs designed with the "convergence-first, diversity-second" search strategy may become ineffective in addressing multiobjective problems with the imbalance feature. In contrast, a search strategy that balances diversity and convergence can enable MOEAs to achieve reasonable performance on these problems. For another example, Li *et al.* [16] proposed using a set of test problems with bias features to study the approximation ability of MOEAs. They concluded that the search scheme combining differential evolution (DE) and covariance matrix adaptation could make MOEAs more efficient in coping with biased multiobjective problems.

In addition to constructing new test problems, the analysis of existing test problems is also imperative [17]. By analyzing and summarizing the features of the test problems, the applicability of each tested MOEA to each problem feature can be understood more clearly. With such clear understanding, more accurate conclusions about the strengths and weaknesses of the algorithms can be drawn [18]. Furthermore, the rigorous analysis of the test problems can contribute to recognizing their design flaws and further refine them. For example, DTLZ5, DTLZ6, and WFG3 were initially built to be multiobjective test problems with degenerate Pareto fronts [18], [19]. However, later studies demonstrated that their Pareto fronts (PFs) are not degenerate when DTLZ5 and DTLZ6 have more than three objectives or WFG3 has more than two objectives [20]–[22]. Constraint conditions introduced in [20]–[22] can be used to remove the nondegenerate parts of their PFs.

The DTLZ test suite proposed by Deb *et al.* [19] is a set of scalable multiobjective test problems. Its first four test problems, DTLZ1–DTLZ4, have frequently been used for the performance evaluation of MOEAs [23]–[29]. However, recently Ishibuchi *et al.* [7] have pointed out that there exist two special characteristics in DTLZ1–DTLZ4, which may lead to unfair comparisons and validations of MOEAs. The two special characteristics can be described as follows.

1) The PFs of DTLZ1–DTLZ4 have regular orientation and are similar to the $(m-1)$-dimensional simplex (see Fig. 2); while the weight/direction vectors of decomposition-based MOEAs are usually also set to be uniformly distributed along the $(m-1)$-dimensional simplex as well (see Fig. 3). This overfitting between

Manuscript received January 15, 2018; revised April 13, 2018; accepted June 1, 2018. Date of publication June 5, 2018; date of current version March 29, 2019. This work was supported by the Data Science and Artificial Intelligence Research Centre, Nanyang Technological University. *(Corresponding author: Zhenkun Wang.)*

Z. Wang and Y.-S. Ong are with the School of Computer Science and Engineering, Nanyang Technological University, Singapore 639798 (e-mail: wangzk@ntu.edu.sg; asysong@ntu.edu.sg).

H. Ishibuchi is with the Department of Computer Science and Engineering, Southern University of Science and Technology, Shenzhen 518055, China (e-mail: hisao@sustc.edu.cn).

This paper has supplementary downloadable material available at http://ieeexplore.ieee.org, provided by the authors. This consists of a PDF file containing some experimental results, such as figures and tables. This material is 927 KB in size.

Color versions of one or more of the figures in this paper are available online at http://ieeexplore.ieee.org.

Digital Object Identifier 10.1109/TEVC.2018.2844286

1089-778X © 2018 IEEE. Personal use is permitted, but republication/redistribution requires IEEE permission.
See http://www.ieee.org/publications_standards/publications/rights/index.html for more information.

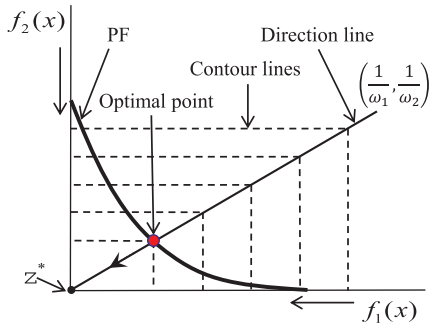

Fig. 1. Illustration of the scalar optimization subproblem defined with the Tchebycheff decomposition method.

the PFs and the distribution of weight/direction vectors facilitates decomposition-based MOEAs to achieve good performance on them.

2) For each of the DTLZ1–DTLZ4 test problems, all the objective functions adopt the same distance function. By only optimizing this single distance function, the Pareto optimal solutions to the problem can be reached. This means that the search for the Pareto optimal solutions is independent of the number of objectives, and more like the single-objective optimization.

In this paper, we first introduce a new set of test problems (denoted as mDTLZ1–mDTLZ4) by modifying DTLZ1–DTLZ4 to avoid the two special characteristics. Using these new test problems, we investigate three representative MOEAs (i.e., NSGA-II, MOEA/D-Tch, and SMS-EMOA), and the results reveal that NSGA-II and MOEA/D-Tch perform poorly on them. By analyzing the feasible region of three-objective mDTLZ1 in the objective space, we find that it has three peculiar boundaries, each of which is connected with one edge of the PF and parallel to a coordinate axis (see Fig. 9). This kind of feasible region boundary, referred to herein as the hardly dominated boundary, causes many difficulties for Pareto dominance-based MOEAs and Tchebycheff-decomposition-based MOEAs. The solutions located on the hardly dominated boundary have the property of dominance resistance, as only a tiny part of solutions in the feasible region can dominate them. They can hardly be replaced or updated by other solutions according to the Pareto dominance criterion and the Tchebycheff decomposition method. Furthermore, we summarize that the hardly dominated boundary should be an often encountered problem feature in multiobjective optimization. Last but not least, we point out and validate some coping strategies for dominance-based MOEAs and decomposition-based MOEAs to overcome the challenges caused by the hardly dominated boundary.

The remainder of this paper proceeds as follows. In Section II, some fundamental concepts are presented along with a brief review of DTLZ1–DTLZ4. In Section III, the new test problems mDTLZ1–mDTLZ4 are introduced in detail. In Section IV, three representative algorithms NSGA-II, MOEA/D-Tch, and SMS-EMOA are tested and compared on the three objective mDTLZ1–mDTLZ4. In Section V, the analysis explains why the performance of Pareto dominance-based MOEAs and Tchebycheff-decomposition-based MOEAs degrades on the mDTLZ1–mDTLZ4 problems. In Section VI, some coping strategies for certain MOEAs are indicated and verified. Some discussions are provided in Section VII. Finally, this paper is concluded in Section VIII.

II. Background

A. Basic Definitions

In general, a continuous multiobjective optimization problem (MOP) can be defined as follows:

$$\begin{aligned} \text{minimize} \quad & \mathbf{f}(\mathbf{x}) = (f_1(\mathbf{x}), \ldots, f_m(\mathbf{x}))^{\mathsf{T}} \\ \text{subject to} \quad & \mathbf{x} \in \Omega \subset \mathbb{R}^n \end{aligned} \tag{1}$$

where $\Omega \subset \mathbb{R}^n$ is the n-dimensional decision space, and $\mathbf{x} = (x_1, \ldots, x_n)^{\mathsf{T}}$ is a decision vector in it. The objective vector $\mathbf{f}(\mathbf{x})$ consisting of m objective functions $\{f_1(\mathbf{x}), \ldots, f_m(\mathbf{x})\}$ defines the mapping from the decision space to the objective space. In this paper, Ω is a closed subset, and all the objective functions are continuous of $\mathbf{x}$.

Definition 1: A solution $\mathbf{x}^1$ is said to *Pareto dominate* another solution $\mathbf{x}^2$, if $f_i(\mathbf{x}^1) \leq f_i(\mathbf{x}^2)$ for all $i \in \{1, \ldots, m\}$, and $f_j(\mathbf{x}^1) < f_j(\mathbf{x}^2)$ for at least one $j \in \{1, \ldots, m\}$.

Definition 2: A solution $\mathbf{x}^*$ is said to be *Pareto optimal*, if there is no other solutions that can Pareto dominate it.

Definition 3: The set of all the Pareto optimal solutions is called the Pareto set (PS), i.e., PS $= \{\mathbf{x}^* \in \Omega | \nexists \mathbf{x} \in \Omega$ dominates $\mathbf{x}^*\}$.

Definition 4: The PF is the set of the images of the solutions in the PS, i.e., PF $= \{\mathbf{f}(\mathbf{x}) | \mathbf{x} \in \text{PS}\}$.

Definition 5: The *ideal point* $\mathbf{z}^* = (z_1^*, \ldots, z_m^*)^{\mathsf{T}}$ is defined as $z_i^* = \min\{f_i(\mathbf{x}) | \mathbf{x} \in \Omega\}$, for $i = 1, \ldots, m$.

Decomposition-based MOEAs decompose an MOP into a set of single objective subproblems and collaboratively optimize them [30]. The Tchebycheff decomposition method is one of the most commonly used decomposition methods, which defines the scalar optimization subproblem as follows:

$$\begin{aligned} \text{minimize} \quad & g\left(\mathbf{x} | \mathbf{w}, \mathbf{z}^*\right) = \max_{1 \leq i \leq m} \left\{ w_i \left| f_i(x) - z_i^* \right| \right\} \\ \text{subject to} \quad & \mathbf{x} \in \Omega \end{aligned} \tag{2}$$

where $\mathbf{w} = (w_1, \ldots, w_m)^{\mathsf{T}}$ is a weight vector that satisfies $w_i \geq 0$ for all $i = 1, \ldots, m$ and $\sum_{i=1}^m w_i = 1$. By using different weight vectors in (2), a set of different scalar optimization subproblems can be achieved. In practice, $w_i = 0$ is replaced by a sufficient small value (e.g., $w_i = 10^{-9}$).

As shown in Fig. 1, the properties of a subproblem defined by (2) can be depicted by a directional line and several contour lines [31], [32]. The intersection between the directional line and the PF is the optimal solution of this subproblem.

B. DTLZ1–DTLZ4 Test Problems

DTLZ1–DTLZ4 are the first four test problems of the DTLZ suite [19]. They can be represented by the following formulation:

$$\text{minimize} \quad f_k(\mathbf{x}) = h_k(\mathbf{x}_I)(1 + g(\mathbf{x}_{II})), \ \text{for } k = 1, \ldots, m \tag{3}$$

where $\mathbf{x} = (x_1, \ldots, x_n)^{\mathsf{T}} \in \Omega$ is the decision vector, $\mathbf{x_I} = (x_1, \ldots, x_{m-1})^{\mathsf{T}}$ and $\mathbf{x_{II}} = (x_m, \ldots, x_n)^{\mathsf{T}}$ are two subvectors of $\mathbf{x}$. $h_1(\mathbf{x}_I), \ldots, h_m(\mathbf{x}_I)$ are usually called the *position functions*, they together define the PF of (3). $g(\mathbf{x}_{II}) \geq 0$ is often called the *distance function*, which determines how far a solution is to the PF. If a solution makes $g(\mathbf{x}_{II})$ to be zero, it would be the Pareto optimal one. The formulations of $g(\mathbf{x}_{II})$

TABLE I
DTLZ1–DTLZ4 TEST PROBLEMS

Problem	Position functions and distance function	Variable domains
DTLZ1	$h_k(\mathbf{x}_I) = \begin{cases} 0.5\prod_{i=1}^{m-1} x_i, & k=1, \\ 0.5\Big(\big(\prod_{i=1}^{m-k} x_i\big)(1-x_{m-k+1})\Big), & k=2,\ldots,m-1, \\ 0.5(1-x_1), & k=m. \end{cases}$ $g(\mathbf{x}_{II}) = 100\Big(n-m+1+\sum_{i=m}^{n}\Big((x_i-0.5)^2 - cos\big(20\pi(x_i-0.5)\big)\Big)\Big).$	$[0,1]^n$
DTLZ2	$h_k(\mathbf{x}_I) = \begin{cases} \prod_{i=1}^{m-1} cos(0.5\pi x_i), & k=1, \\ \big(\prod_{i=1}^{m-k} cos(0.5\pi x_i)\big) sin(0.5\pi x_{m-k+1}), & k=2,\ldots,m-1, \\ sin(0.5\pi x_1), & k=m. \end{cases}$ $g(\mathbf{x}_{II}) = \sum_{i=m}^{n}\Big((x_i-0.5)^2\Big).$	$[0,1]^n$
DTLZ3	$h_k(\mathbf{x}_I)$ for $k=1,\ldots,m$ are the same as those in DTLZ2. $g(\mathbf{x}_{II})$ is the same as that in DTLZ1.	$[0,1]^n$
DTLZ4	$h_k(\mathbf{x}_I) = \begin{cases} \prod_{i=1}^{m-1} cos(0.5\pi x_i^{100}), & k=1, \\ \big(\prod_{i=1}^{m-k} cos(0.5\pi x_i^{100})\big) sin(0.5\pi x_{m-k+1}^{100}), & k=2,\ldots,m-1, \\ sin(0.5\pi x_1^{100}), & k=m. \end{cases}$ $g(\mathbf{x}_{II}) = \sum_{i=m}^{n}\Big((x_i^{100}-0.5)^2\Big).$	$[0,1]^n$

and $(h_1(\mathbf{x}_I),\ldots,h_m(\mathbf{x})_I)^\intercal$ in DTLZ1–DTLZ4 are presented in Table I.

As shown in Table I, let $\mathbf{y}^* = (y_1^*,\ldots,y_m^*)^\intercal$ be a Pareto optimal solution in the objective space, the PFs of DTLZ1–DTLZ4 can be represented by the following formulations:

$$\text{DTLZ1:} \quad \sum_{i=1}^{m} y_i^* = 0.5, \quad 0 \le y_i^* \le 0.5 \text{ for } i=1,\ldots,m \tag{4}$$

$$\text{DTLZ2-DTLZ4:} \quad \sum_{i=1}^{m} (y_i^*)^2 = 1, \quad 0 \le y_i^* \le 1 \text{ for } i=1,\ldots,m. \tag{5}$$

The PFs of three-objective DTLZ1–DTLZ4 are illustrated in Fig. 2. It can be observed that the shape of each problem's PF is the same or similar to the shape of the 2-D simplex (i.e., triangular plane).

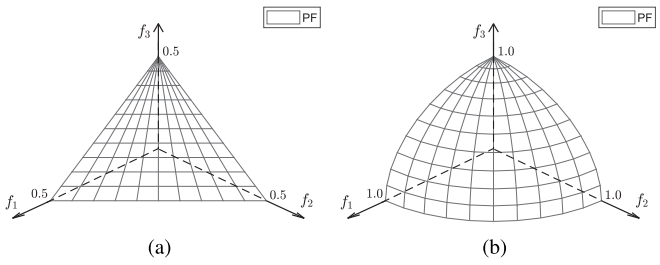

Fig. 2. PFs of DTLZ1–DTLZ4 with three objectives. (a) DTLZ1. (b) DTLZ2–DTLZ4.

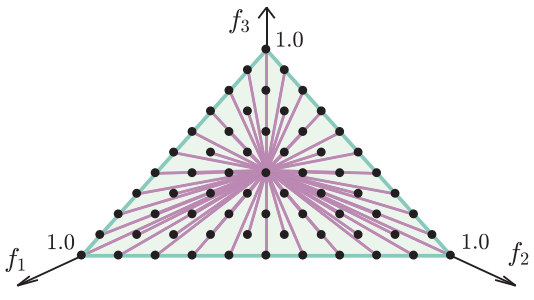

Fig. 3. Distribution of weight/direction vectors used in decomposition-based MOEAs.

C. Two Special Characteristics

Although the DTLZ1–DTLZ4 problems are one of the most popular benchmark problems in evolutionary multiobjective optimization research, they have recently been identified as less general due to their two special characteristics [7].

1) Regularly Oriented PF Shape: The PFs of DTLZ1–DTLZ4 have regular orientation and their shapes are similar to the shape of the $(m-1)$-dimensional simplex (see Fig. 2). However, the weight/direction vectors of decomposition-based MOEAs are usually set to be uniformly distributed along the $(m-1)$-dimensional simplex (see Fig. 3) as well. There is an over-fitting between their PF shapes and the distribution of the weight/direction vectors, which naturally helps decomposition-based MOEAs in achieving a set of well-distributed approximate solutions. As benchmark test

TABLE II
MDTLZ1–MDTLZ4 TEST PROBLEMS

Problem	Position functions and distance functions	Variable domains
mDTLZ1	$h_k(\mathbf{x}_I) = \begin{cases} 0.5\big(1-\prod_{i=1}^{m-1} x_i\big), & k=1, \\ 0.5\Big(1-\big(\prod_{i=1}^{m-k} x_i\big)(1-x_{m-k+1})\Big), & k=2,\ldots,m-1, \\ 0.5x_1, & k=m. \end{cases}$ $g_k(\mathbf{x}_{II}) = 100\Big(\lvert\phi_k\rvert + \sum_{i\in\phi_k}\Big((x_i-0.5)^2 - cos\big(20\pi(x_i-0.5)\big)\Big)\Big)$, where $\phi_k = \{m-1+k, 2m-1+k, \ldots, \lfloor\frac{n+1-k}{m}\rfloor m-1+k\}$ for $k=1,\ldots,m$.	$[0,1]^n$
mDTLZ2	$h_k(\mathbf{x}_I) = \begin{cases} 1-\prod_{i=1}^{m-1} cos(0.5\pi x_i), & k=1, \\ 1-\big(\prod_{i=1}^{m-k} cos(0.5\pi x_i)\big) sin(0.5\pi x_{m-k+1}), & k=2,\ldots,m-1, \\ 1-sin(0.5\pi x_1), & k=m. \end{cases}$ $g_k(\mathbf{x}_{II}) = \sum_{i\in\phi_k}\Big((x_i-0.5)^2\Big)$, where $\phi_k = \{m-1+k, 2m-1+k, \ldots, \lfloor\frac{n+1-k}{m}\rfloor m-1+k\}$ for $k=1,\ldots,m$.	$[0,1]^n$
mDTLZ3	$h_k(\mathbf{x}_I)$ for $k=1,\ldots,m$ are the same as those in mDTLZ2. $g_k(\mathbf{x}_{II})$ are the same as those in mDTLZ1.	$[0,1]^n$
mDTLZ4	$h_k(\mathbf{x}_I) = \begin{cases} 1-\prod_{i=1}^{m-1} cos(0.5\pi x_i^{100}), & k=1, \\ 1-\big(\prod_{i=1}^{m-k} cos(0.5\pi x_i^{100})\big) sin(0.5\pi x_{m-k+1}^{100}), & k=2,\ldots,m-1, \\ 1-sin(0.5\pi x_1^{100}), & k=m. \end{cases}$ $g_k(\mathbf{x}_{II}) = \sum_{i\in\phi_k}\Big((x_i^{100}-0.5)^2\Big)$, where $\phi_k = \{m-1+k, 2m-1+k, \ldots, \lfloor\frac{n+1-k}{m}\rfloor m-1+k\}$ for $k=1,\ldots,m$.	$[0,1]^n$

problems, such an over-fitting should be avoided so as to provide fair comparisons of MOEAs.

2) Single Distance Function: For each of the DTLZ1–DTLZ4 test problems, all the objective functions employ the same distance function. In this case, if a solution $\mathbf{x}^1$ is better than another solution $\mathbf{x}^2$ with respect to this single distance function (the values of the position functions are the same), then $\mathbf{x}^1$ can dominate $\mathbf{x}^2$ [see Fig. 6(a)]. That is, the Pareto optimal solutions can be obtained by merely optimizing the single distance function. This means that the search for the Pareto optimal solutions is independent of the number of objectives, and more like a single-objective optimization.

III. MODIFIED DTLZ PROBLEMS

To avoid the two special characteristics, in this section, we introduce the modified variants of the DTLZ1–DTLZ4 problems (denoted as mDTLZ1–mDTLZ4). Besides, we provide some analysis and experiments in this section to illustrate that the mDTLZ1–mDTLZ4 test problems can get rid of the two special characteristics.

A. mDTLZ1–mDTLZ4 Test Problems

The mDTLZ1–mDTLZ4 test problems can be written in the following form:

$$\text{minimize } f_k(\mathbf{x}) = h_k(\mathbf{x}_I)(1+g_k(\mathbf{x}_{II})), \text{ for } k=1,\ldots,m \tag{6}$$

where the definitions of $\mathbf{x}$, $\mathbf{x}_I$, and $\mathbf{x}_{II}$ are the same as in (3). Note that each objective function $f_k \in \{f_1,\ldots,f_m\}$ in (6) employs a distinct distance function g_k. The formulations of g_k and h_k in mDTLZ1–mDTLZ4 are shown in Table II.

As shown in Table II, if we let $\mathbf{y}^* = (y_1^*,\ldots,y_m^*)^\intercal$ be a Pareto optimal solution in the objective space, the PFs of mDTLZ1–mDTLZ4 can be expressed by the following formulations:

$$\text{mDTLZ1:} \quad \sum_{i=1}^{m} y_i^* = 0.5(m-1), \quad 0 \le y_i^* \le 0.5 \text{ for } i=1,\ldots,m \tag{7}$$

$$\text{mDTLZ2-mDTLZ4:} \quad \sum_{i=1}^{m}\big(y_i^*-1\big)^2 = 1, \quad 0 \le y_i^* \le 1 \text{ for } i=1,\ldots,m. \tag{8}$$

Fig. 4 illustrates the PFs of three-objective mDTLZ1–mDTLZ4. It can be found that the PF shapes of mDTLZ1–mDTLZ4 are similar to the shape of the inverted 2-D simplex (i.e., inverted triangular plane).

B. PF Shapes and Distance Functions

Similar to the DTLZ^{-1} test problems [7], the PF shapes with inverted orientation are adopted in mDTLZ1–mDTLZ4. Multiobjective test problems with such PF shapes can evade several undesirable features. For example, as discussed

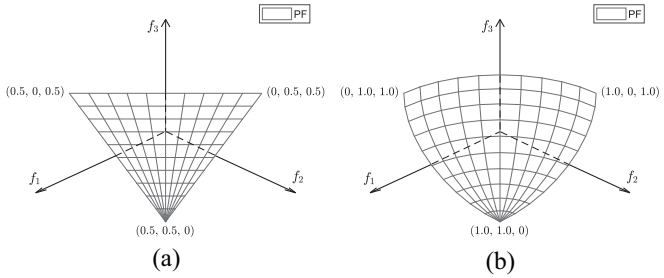

Fig. 4. PFs of three-objective mDTLZ1–mDTLZ4. (a) mDTLZ1. (b) mDTLZ2–mDTLZ4.

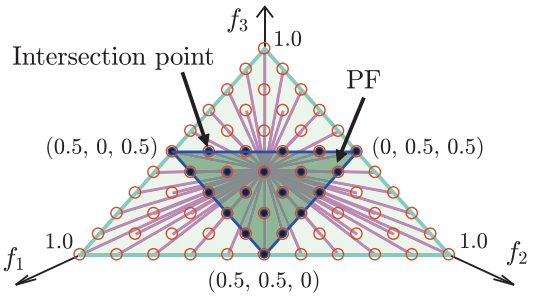

Fig. 5. Relation between weight/direction vectors and the PF of mDTLZ1.

in [33] and [34], there is a problematic and unrealistic feature in the m-objective test problems whose PFs are similar to the regular $(m-1)$-dimensional simplex (e.g., DTLZ1–DTLZ4 and WFG4–WFG9). To illustrate it, let us first consider a practical example of multiobjective optimization in buying a car. When choosing a car, we often consider several conflicting criteria or objectives (e.g., minimizing price, maximizing comfort, maximizing engine performance, and minimizing fuel consumption). With respect to minimizing price and maximizing engine performance, the optimization would involve two conflicting metrics (i.e., price and engine performance). Thus, there exists a set of tradeoff solutions are optimal in a nondominated sense. However, the nature of the test problems with regularly oriented PFs cannot fulfill with this property of the contradiction between the objectives. This is because this kind of test problem has a feature that its any $(m-1)$ objectives are nonconflicting to each other, i.e., there exists a single solution can simultaneously optimize its any $(m-1)$ objective functions. In other words, the PF degenerates into a single point if we arbitrarily omit one objective of the test problem. On the other hand, the mDTLZ problem can address such a shortcoming so that the optimization involving any k objective functions $(1 < k < m)$ results in a set of tradeoff solutions rather than a single solution. Furthermore, mDTLZ1–mDTLZ4 can avoid being over-friendly to decomposition-based algorithms since their PFs no longer exactly match the distribution of the weight/direction vectors (see Fig. 5).

Referring to [7], we conduct a comparative experiment on DTLZ1 and mDTLZ1 to illustrate their distance function related properties. As shown in Fig. 6(a) and (b), we first randomly generate an initial solution (shown as a hexagram) on DTLZ1 and mDTLZ1, respectively. Then we generate 100 child solutions (shown as circles) from each initial solution by randomly changing the values of its distance related variables (i.e., $x_m, \ldots, x_n$). That is, we keep the initial solution's position

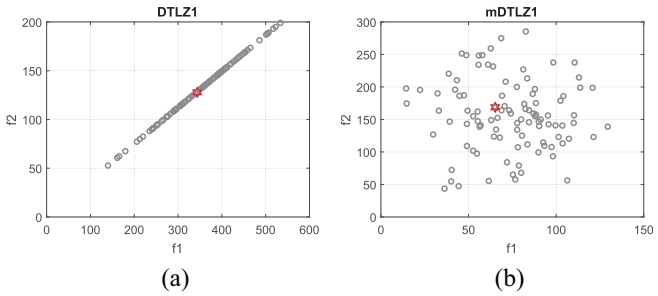

Fig. 6. One hundred solutions generated by randomly changing the initial solution's distance related variables on two-objective DTLZ1 and mDTLZ1, respectively. (a) DTLZ1. (b) mDTLZ1.

related variables (i.e., $x_1, \ldots, x_{m-1}$) unchanged and replace its position related variables with randomly generated values within their domains. It can be seen that the solutions generated on DTLZ1 are all located on a straight line [see Fig. 6(a)]. This is mainly because all the objective functions of DTLZ1 use the same distance function. In this case, the solutions that differ only on this single distance function are surely on the same line. In other words, the Pareto optimal solutions can be achieved by optimizing only the single distance function. This means that the search for the Pareto optimal solutions is single-objective optimization. However, such a phenomenon is not shown in Fig. 6(b) since each objective function of mDTLZ1 adopts a distinct distance function.

Overall, it can be concluded that mDTLZ1–mDTLZ4 can avoid the two special characteristics, i.e., the regularly oriented PF shape and the single distance function. Next, one might wonder if existing MOEAs are still effective on mDTLZ1–mDTLZ4.

IV. Experimental Testing

In this section, three representative MOEAs, NSGA-II [35], MOEA/D-Tch [30], and SMS-EMOA [36], are tested and compared on three-objective mDTLZ1–mDTLZ4.

A. Examined Algorithms and Parameter Settings

1) NSGA-II is a classical dominance-based MOEA, which employs the Pareto dominance criterion and the crowding distance for fitness evaluation.
2) MOEA/D-Tch is a commonly used decomposition-based MOEA. By adopting a group of uniformly distributed weight vectors in the Tchebycheff decomposition method, MOEA/D-Tch decomposes an MOP into a set of single objective optimization subproblems and optimizes them collaboratively.
3) SMS-EMOA is a well-known indicator-based MOEA that uses the hypervolume (HV) metric for population diversity maintenance.

The parameters of NSGA-II, MOEA/D-Tch, and SMS-EMOA are set according to their corresponding references, respectively [30], [35], and [36]. To have a fair comparison, we let three MOEAs use the same reproduction procedure (i.e., the simulated binary crossover and the polynomial mutation) for the generation of offspring solutions. The detailed parameter settings are summarized as follows.

1) *Number of Objectives and Decision Variables:* All three algorithms are performed on mDTLZ1–mDTLZ4 with $m = 3$ and $n = 10$.

TABLE III
Δ_2-METRIC VALUES OBTAINED BY NSGA-II, MOEA/D-TCH, AND SMS-EMOA ON THE THREE-OBJECTIVE MDTLZ1–MDTLZ4

Δ_2	NSGA-II			MOEA/D-Tch			SMS-EMOA		
Problem		Median	Best		Median	Best		Median	Best
mDTLZ1	3−	1.739E+02	1.586E+02	2−	2.360E+01	1.414E+01	**1**	**1.699E-02**	**1.667E-02**
mDTLZ2	3−	3.432E-01	3.334E-01	2−	6.285E-02	6.096E-02	**1**	**3.665E-02**	**3.598E-02**
mDTLZ3	3−	3.427E+02	3.286E+02	2−	5.111E+01	4.153E+01	**1**	**3.702E-02**	**3.610E-02**
mDTLZ4	3−	3.459E-01	3.308E-01	2−	2.887E-01	2.394E-01	**1**	**3.689E-02**	**3.631E-02**

$+$,$-$ and $\approx$ denote that the performance of the corresponding algorithm is significantly better than, worse than, and similar to SMS-EMOA respectively by Wilcoxon's rank sum test with $\alpha = 0.05$.

TABLE IV
HV-METRIC VALUES OBTAINED BY NSGA-II, MOEA/D-TCH, AND SMS-EMOA ON THE THREE-OBJECTIVE MDTLZ1–MDTLZ4

HV	NSGA-II			MOEA/D-Tch			SMS-EMOA		
Problem		Median	Best		Median	Best		Median	Best
mDTLZ1	3−	0.58775	0.83269	2−	1.34773	1.34860	**1**	**1.35351**	**1.35355**
mDTLZ2	3−	0.96562	0.97986	2−	1.05960	1.06082	**1**	**1.07938**	**1.07961**
mDTLZ3	3−	0	0.05199	2−	1.05331	1.05593	**1**	**1.07890**	**1.07929**
mDTLZ4	3−	0.94384	0.96860	2−	0.98874	1.05315	**1**	**1.07901**	**1.07925**

$+$,$-$ and $\approx$ denote that the performance of the corresponding algorithm is significantly better than, worse than, and similar to SMS-EMOA respectively by Wilcoxon's rank sum test with $\alpha = 0.05$.

2) *Population Size:* The population size is set to be 300 for each algorithm. That is, $N = 300$ for NSGA-II and SMS-EMOA, and $H = 23$ for MOEA/D-Tch.
3) *Number of Runs and Stopping Condition:* Each algorithm is carried out 30 times independently for each test problem. In each run, the algorithm terminates when the maximal number of function evaluation reaches 100 000.
4) *Settings for Reproduction Operators:* The distribution indexes in the simulated binary crossover and the polynomial mutation are set to be 15 and 20, respectively. The crossover probability is 0.9, and the mutation probability is 0.1.

B. Performance Metrics

In our experiments, the Δ_p indicator and the HV indicator are used to assess the performance of the comparison algorithms.

1) *Δ_p-Metric [37]:* Let Q be a set of uniformly distributed Pareto optimal solutions in the objective space. Let S be an approximate set obtained by the algorithm. Then $\Delta_p(Q, S)$ is defined as

$$\Delta_p(Q, S) = \max\{GD_p(Q, S), IGD_p(Q, S)\} \tag{9}$$

where

$$GD_p(Q, S) = \left(\frac{\sum_{\mathbf{u}\in S} \text{dist}(\mathbf{u}, Q)^p}{|S|}\right)^{\frac{1}{p}} \tag{10}$$

$$IGD_p(Q, S) = \left(\frac{\sum_{\mathbf{v}\in Q} \text{dist}(\mathbf{v}, S)^p}{|Q|}\right)^{\frac{1}{p}}. \tag{11}$$

For a solution $\mathbf{u}$ and a solution set A, $\text{dist}(\mathbf{u}, A)$ is defined as follows:

$$\text{dist}(\mathbf{u}, A) = \inf_{\mathbf{v}\in A} \|\mathbf{u} - \mathbf{v}\| \tag{12}$$

where $\|\cdot\|$ is the vector norm. In this paper, we use 2-norm for $\text{dist}(\cdot, \cdot)$. Furthermore, we let $p = 2$ and choose 1000 representative points to approximate Q for each three-objective test problem.

2) *HV-Metric [38]:* Let $\mathbf{y}^* = (y_1^*, y_2^*, \ldots, y_m^*)^\intercal$ be a reference point that satisfies $y_i^* \geq \max_{\mathbf{x}\in \text{PS}} f_i(\mathbf{x})$. The HV-metric value of the approximate set S against $\mathbf{y}^*$ is the volume of the region between S and $\mathbf{y}^*$, which is computed by

$$I_H(S, y^*) = \text{vol}\left(\bigcup_{\mathbf{y}\in S} [y_1, y_1^*] \times \ldots \times [y_m, y_m^*]\right) \tag{13}$$

where $\text{vol}(\cdot)$ is the Lebesgue measure. In our experiments, $\mathbf{y}^* = (1.2, 1.2, 1.2)^\intercal$ is used for all three-objective test problems.

C. Experimental Results

Experimental results obtained by three MOEAs in terms of the Δ_2-metric and the HV-metric are shown in Tables III and IV, respectively. Moreover, the statistical significance results and the rankings of algorithms are also provided in both tables. Furthermore, Fig. 7 plots the obtained final solutions which have the median Δ_2-metric values from each algorithm's 30 runs on mDTLZ1–mDTLZ4. These results indicate that SMS-EMOA significantly outperforms NSGA-II and MOEA/D-Tch on all four problems. By contrast, MOEA/D-Tch performs better than NSGA-II. As shown in Fig. 7(a), NSGA-II fails to approximate the PFs of mDTLZ1 and mDTLZ3, as the solutions it attains are far away from the PFs. For mDTLZ2 and mDTLZ4, although NSGA-II can find some solutions on the theoretical PFs, it also retains many other nondominated solutions in the final population. In Fig. 7(b), it shows that the vast majority of the solutions achieved by MOEA/D-Tch are located on the theoretical PFs. Nevertheless, MOEA/D-Tch still keeps some undesirable solutions in the approximate sets, especially for mDTLZ1 and

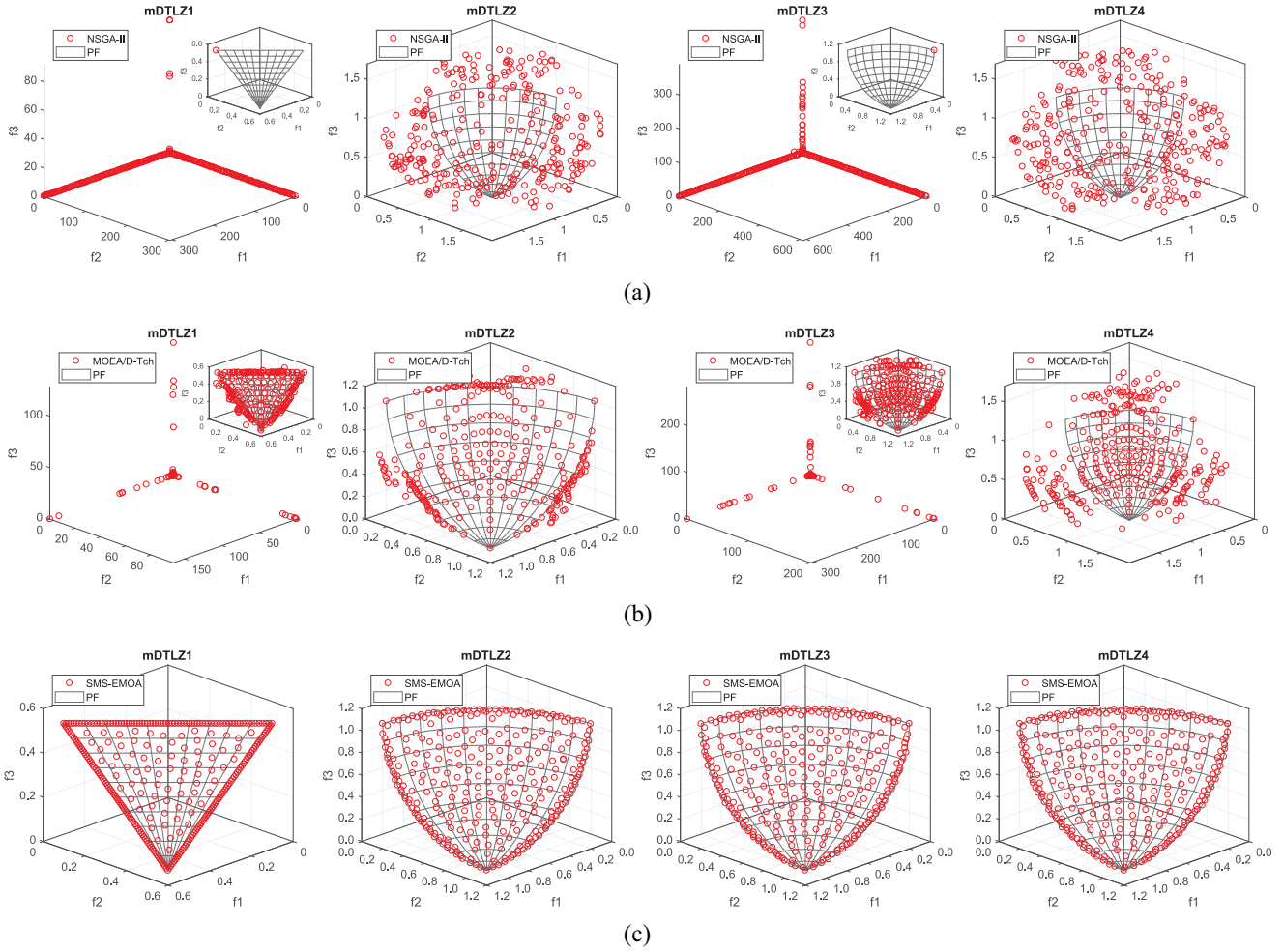

Fig. 7. Plots of the final solutions with the median Δ_2-metric values found by three MOEAs in 30 runs on the three-objective mDTLZ1–mDTLZ4. (a) NSGA-II. (b) MOEA/D-Tch. (c) SMS-EMOA.

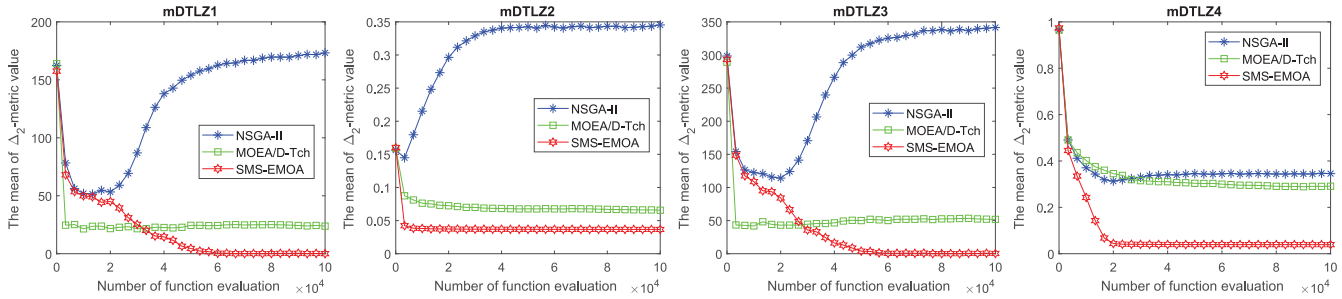

Fig. 8. Evolution of the mean Δ_2-metric values of three MOEAs on the three-objective mDTLZ1–mDTLZ4.

mDTLZ3. On the other hand, Fig. 7(c) indicates that the solutions gained by SMS-EMOA can well approximate the PFs of mDTLZ1–mDTLZ4.

Fig. 8 presents the evolution of the mean Δ_2-metric values of three algorithms on each problem versus the number of function evaluations. It is evident that SMS-EMOA is more effective and efficient than MOEA/D-Tch and NSGA-II in reducing the Δ_2-metric values on all four test problems. MOEA/D-Tch also can gradually reduce the Δ_2-metric values, but not as efficiently as SMS-EMOA. NSGA-II cannot achieve satisfying Δ_2-metric results on any mDTLZ problem. The obtained mean Δ_2-metric value is even getting worse with the number of function evaluations.

In summary, only the HV indicator-based algorithm SMS-EMOA can achieve satisfactory results on mDTLZ1–mDTLZ4. The performance of the Pareto dominance-based algorithm NSGA-II is severely deteriorated on these four MOPs. The Tchebycheff-decomposition-based algorithm MOEA-Tch is also plagued by the undesirable solutions in the final approximate sets. In the following, we will explain the reasons for the performance deterioration of Pareto dominance-based MOEAs and Tchebycheff-decomposition-based MOEAs in dealing with MOPs like mDTLZ1–mDTLZ4.

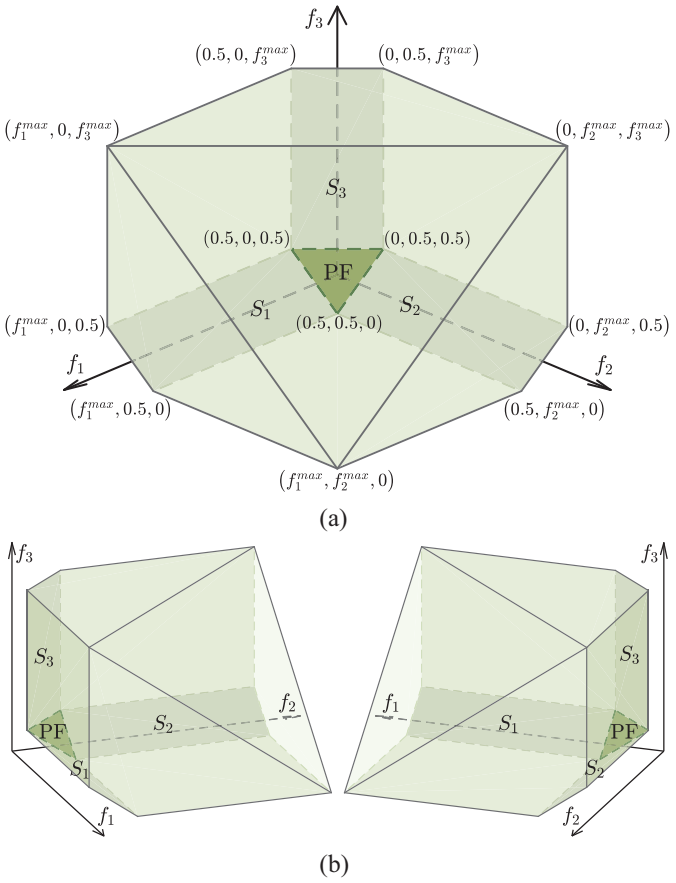

Fig. 9. Feasible region of three-objective mDTLZ1 is illustrated with (a) detailed information as well as shown from two (b) other perspectives.

V. Analysis

In this section, we take three-objective mDTLZ1 as an example to explain why Pareto dominance-based MOEAs and Tchebycheff-decomposition-based MOEAs are less effective on the mDTLZ problems. In Fig. 9, we illustrate the feasible region of mDTLZ1 in the objective space. $f_i^{\max}$ in Fig. 9(a) represents the maximum value of the ith objective function of mDTLZ1, i.e., $f_i^{\max} = \max\{f_i(\mathbf{x})|\mathbf{x} \in \Omega\}$, for $i = 1, \ldots, m$. In Table V, we also provide the formulas for calculating the maximum values of the objective functions for each DTLZ and mDTLZ problem. If the parameter settings are the same as in Section IV (i.e., $m = 3$, $n = 10$, $\phi_1 = \{3, 6, 9\}$, $\phi_2 = \{4, 7, 10\}$, and $\phi_3 = \{5, 8\}$), it can be deduced that $f_1^{\max} = f_2^{\max} = 330.875$ and $f_3^{\max} = 220.75$ in mDTLZ1.

It can be observed from Fig. 9 that the feasible region of mDTLZ1 has three peculiar boundaries (i.e., plane S_1, plane S_2, and plane S_3), each of which is connected to one edge of the PF and parallel to one of the coordinate axes. In combination with the results in Fig. 7, it appears that the undesirable solutions acquired by NSGA-II and MOEA/D-Tch are mainly located on these three boundaries. Thus, we infer that these peculiar boundaries may be responsible for the performance degradation of the two algorithms. This type of feasible region boundary is referred to as the hardly dominated boundary in this paper. Let $\mathbf{y} = (y_1, \ldots, y_m)^\intercal$ be an objective vector on the hardly dominated boundaries, the ith ($i = 1, \ldots, m$) hardly dominated boundary of each mDTLZ problem can be represented as follows:

TABLE V
Maximum Values of the Objective Functions in DTLZ1–DTLZ4 and mDTLZ1–mDTLZ4

Problem	Maximum values of the objective functions
DTLZ1	$f^{max}_{i=1,\ldots,m} = 110.125(n-m) + 110.625.$
DTLZ2	$f^{max}_{i=1,\ldots,m} = 0.25(n-m) + 1.25.$
DTLZ3	$f^{max}_{i=1,\ldots,m} = 220.25(n-m) + 221.25.$
DTLZ4	Same as DTLZ2.
mDTLZ1	$f^{max}_{i=1,\ldots,m} = 110.125\lvert\phi_i\rvert + 0.5.$
mDTLZ2	$f^{max}_{i=1,\ldots,m} = 0.25\lvert\phi_i\rvert + 1.$
mDTLZ3	$f^{max}_{i=1,\ldots,m} = 220.25\lvert\phi_i\rvert + 1.$
mDTLZ4	Same as mDTLZ2.

$$\text{mDTLZ1:}\quad \begin{aligned} &\sum_{j\in\Psi_i} y_j = 0.5(m-2)\\ &0 \le y_j \le 0.5 \text{ for } j \in \Psi_i\\ &0.5 < y_j \le f_i^{\max} \text{ for } j = i\\ &\Psi_i = \{1, \ldots, m\} \setminus \{i\} \end{aligned} \tag{14}$$

$$\text{mDTLZ2-mDTLZ4:}\quad \begin{aligned} &\sum_{j\in\Psi_i} \big(y_j - 1\big)^2 = 1\\ &0 \le y_j \le 1 \text{ for } j \in \Psi_i\\ &1 < y_j \le f_i^{\max} \text{ for } j = i\\ &\Psi_i = \{1, \ldots, m\} \setminus \{i\}. \end{aligned} \tag{15}$$

In the following, we explain how the hardly dominated boundary hinders the approximation of Pareto dominance-based MOEAs and Tchebycheff-decomposition-based MOEAs, respectively.

A. Pareto Dominance-Based MOEA Versus MOP With Hardly Dominated Boundaries

In fact, the solutions on the hardly dominated boundaries can be recognized as dominance resistant solutions (DRSs) since they have the property of dominance resistance [39], [40]. The DRSs can cause Pareto dominance-based MOEAs difficulty in approximating the PF [19], [41]. Fig. 10 demonstrates this matter with three-objective mDTLZ1 as an example. D and F in the figure are two solutions on the third hardly dominated boundary (parallel to f_3-axis). E and G are two Pareto optimal solutions which have the same f_1 and f_2 values with D and F, respectively. As we can see in Fig. 10, the solution D (F) can only be dominated by the solutions located on the line segment DE (FG). However, such solutions are scarcely able to find by an MOEA. That is, the solutions on the hardly dominated boundaries are very likely to be identified by Pareto dominance-based MOEAs as nondominated solutions, even they are far away from the PF. In this case, Pareto dominance-based MOEAs will select and maintain many diverse solutions on the hardly dominated boundaries under the action of niche strategies (e.g., crowding distance).

If the hardly dominated boundaries have a much larger size than the PF, Pareto dominance-based MOEAs will prefer

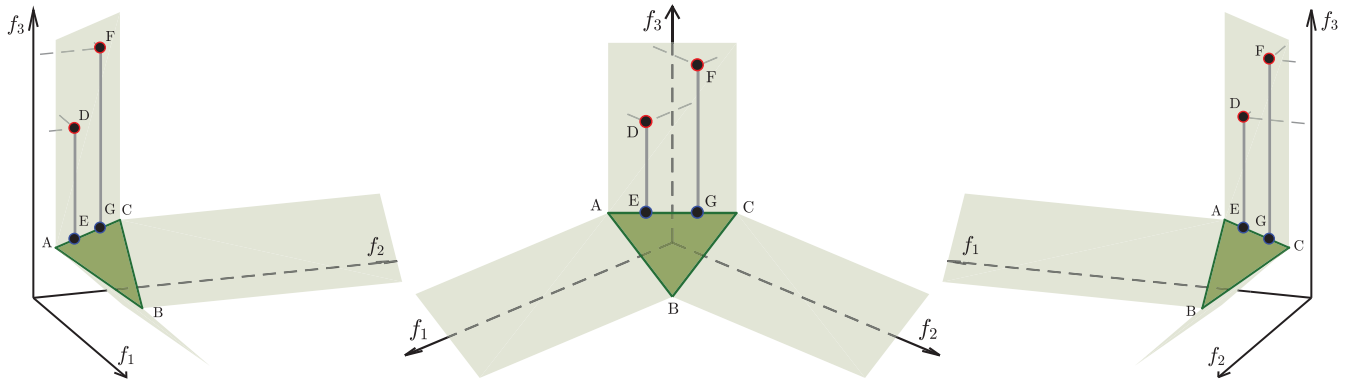

Fig. 10. Multiperspective illustration of the Pareto dominance relation of two solutions which lie on the hardly dominated boundary of mDTLZ1.

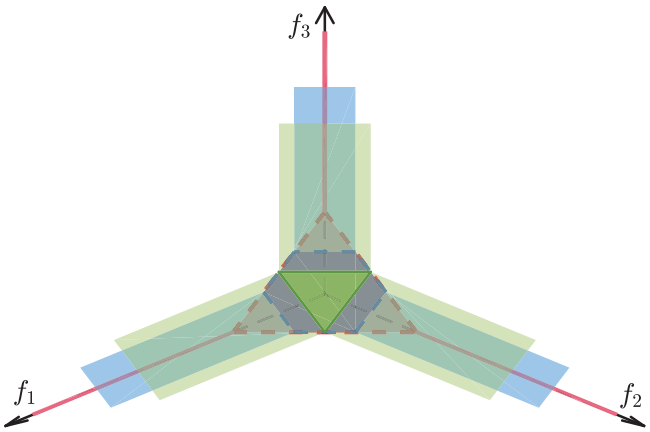

Fig. 11. Three different PF shapes and their corresponding hardly dominated boundaries.

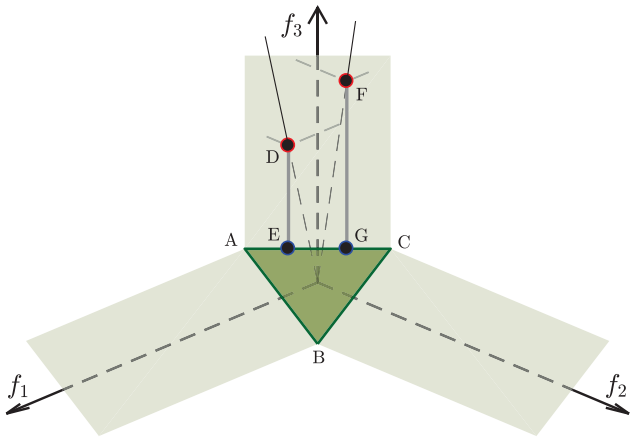

Fig. 12. Illustration of two subproblems whose direction lines across the hardly dominated boundary of mDTLZ1.

to maintain nondominated solutions on the hardly dominated boundaries rather than the PF. It is because the nondominated solutions on the hardly dominated boundaries can be more diverse than the solutions on the PF. This explains why NSGA-II performs worse on mDTLZ1 and mDTLZ3 than on mDTLZ2 and mDTLZ4 [see Fig. 7(a)]. The hardly dominated boundaries of mDTLZ1 and mDTLZ3 are much larger than those boundaries of mDTLZ2 and mDTLZ4. The sizes of the hardly dominated boundaries of each mDTLZ problem are mainly determined by the maximum values of the objective functions (i.e., $f_1^{\max}, \ldots, f_m^{\max}$ in Table V). If $f_i^{\max}$ has a larger value, its corresponding ith hardly dominated boundary will have a greater "length" and thus a larger size.

In addition, the PF shape can also affect the sizes of the hardly dominated boundaries. To explain this, we illustrate three different PF shapes and their corresponding hardly dominated boundaries in Fig. 11. It can be seen that the PF shape limits the "widths" of the hardly dominated boundaries. For example, when the PF adopts a hexagonal shape [34] rather than an inverted triangular shape, the corresponding hardly dominated boundaries have smaller widths. However, when the PF uses a triangular shape, each hardly dominated boundary degenerates to a line (i.e., each axis with the width of zero). This may explain why Pareto dominance-based MOEAs have rarely encountered the challenges posed by the hardly dominated boundaries when dealing with the DTLZ problems.

B. Tchebycheff-Decomposition-Based MOEA Versus MOP With Hardly Dominated Boundaries

In Fig. 12, we illustrate two example subproblems of a Tchebycheff-decomposition-based MOEA, whose direction lines cross the third hardly dominated boundary (parallel to f_3-axis) rather than the PF of mDTLZ1. The intersection points are shown by points D and F in the figure. E and G are two Pareto optimal solutions which have the same f_1 and f_2 values with D and F, respectively. From the figure, we can find that the optimal solution to each of such subproblems is not unique. For example, all the solutions on the line segment DE (FG) can make the corresponding subproblem to be optimal. In this case, once a solution on the line segment DE (FG) except E (G) is obtained during the search, the subproblem cannot be further improved. The subproblem will keep this solution and finally output it as an approximate solution. Since many subproblems' direction lines intersect with the hardly dominated boundaries instead of the PF (see Fig. 5), the algorithm may yield quite a number of solutions on the hardly dominated boundaries rather than on the PF [see Fig. 7(b)].

From Fig. 7(b), we can observe that the performance of MOEA/D-Tch is also affected by the sizes of the hardly dominated boundaries. The larger the hardly dominated boundaries of the problems (e.g., mDTLZ1 and mDTLZ3), the worse the performance achieved by MOEA/D-Tch.

When a Tchebycheff-decomposition-based MOEA deals with the DTLZ problems, all the subproblems' direction lines

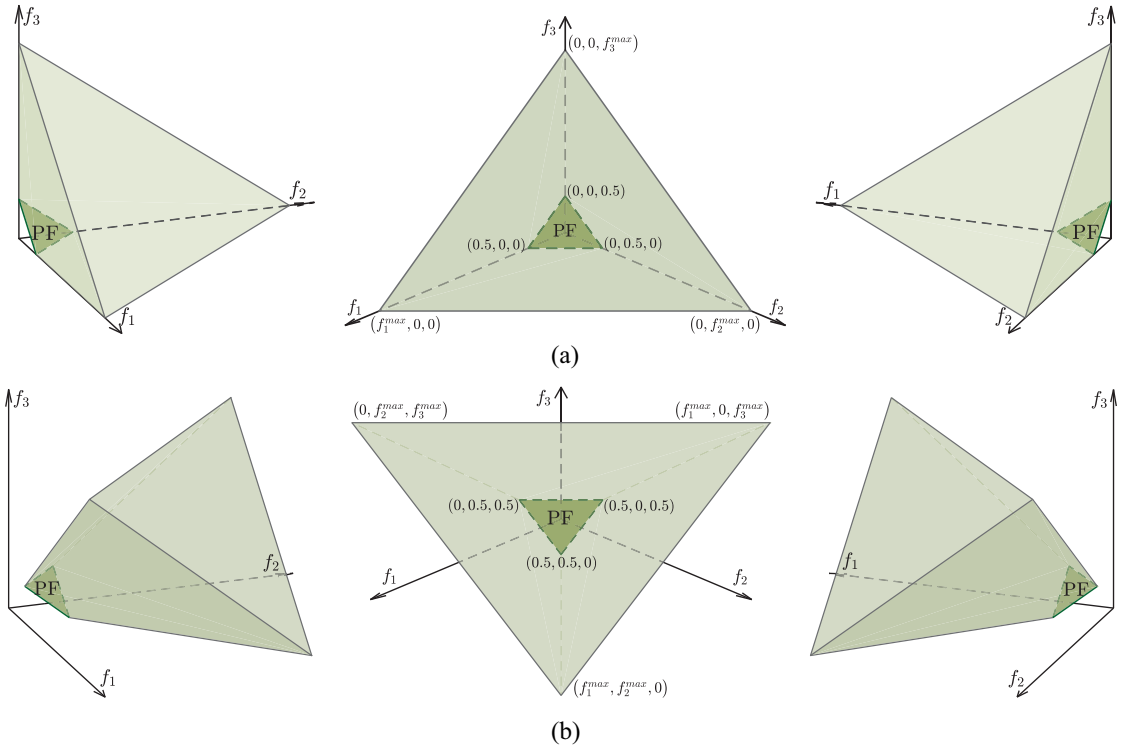

Fig. 13. Feasible regions of (a) mDTLZ1-V1 and (b) mDTLZ1-V2.

have intersections with the PF. Meanwhile, each of these subproblems has a unique optimal solution. In such situations, the subproblems will not suffer from the hindrances of nonunique optimal solutions, and thereby the algorithm can perform well.

C. Influence of Each Modification

Since there are two modifications in the mDTLZ problem (one for the PF shape and the other for the distance function), it is unclear how each part affects the features of the test problem. To illustrate them, we develop two variants of mDTLZ1. They are denoted as mDTLZ1-V1 and mDTLZ1-V2, respectively. In mDTLZ1-V1, we use the regularly oriented PF shape but different distance functions. That is, we replace the position functions (i.e., $h_1, \ldots, h_m$) of mDTLZ1 with the position functions of DTLZ1. In mDTLZ1-V2, we adopt the inverted PF shape and single distance function, i.e., we let $g_k = g$ for $k \in \{1, \ldots, m\}$, where $g_1, \ldots, g_m$ are the distance functions of mDTLZ1 and g is the distance function of DTLZ1. For both mDTLZ1-V1 and mDTLZ1-V2, we set $m = 3$ and $n = 8$.

The three MOEAs set with the same parameters as in Section IV are performed on mDTLZ1-V1 and mDTLZ1-V2. The solutions obtained by three algorithms with the median Δ_2-metric values are shown in Fig. 19 in the supplementary material. Moreover, the evolution of their mean Δ_2-metric values with the number of function evaluations is exhibited in Fig. 20 in the supplementary material. These results clearly show that all three algorithms can get reasonably good results on mDTLZ1-V1 and mDTLZ1-V2. To explain the reasons behind these results, we provide the feasible regions of mDTLZ1-V1 and mDTLZ1-V2 in Fig. 13. It can be seen from Fig. 13(a) that the hardly dominated boundaries of mDTLZ1-V1 degenerate into three lines (i.e., three axes). As discussed earlier, algorithms encounter few related challenges when the hardly dominated boundaries are tiny. From Fig. 13(b), it can be found that the boundaries of mDTLZ1-V2's feasible region are not parallel to the axes. In other words, there is no hardly dominated boundary in the feasible region of mDTLZ1-V2. Without the challenges caused by the hardly dominated boundary, NSGA-II and MOEA/D-Tch could perform well on mDTLZ1-V1 and mDTLZ1-V2.

D. Existence Conditions of the Hardly Dominated Boundary

Although the hardly dominated boundary can pose many difficulties for certain MOEAs, one may wonder whether it is a common problem feature of multiobjective optimization. In the following, the conditions for the existence of the hardly dominated boundary in an MOP are provided.

Definition 6: An MOP is featured with the *hardly dominated boundary*, if there exists at least one $f_i \in \{f_1, \ldots, f_m\}$ that satisfies the following.

1) The minimization of $\{f_1, \ldots, f_m\} \setminus \{f_i\}$ is a set of tradeoff solutions rather than a single solution.
2) These tradeoff solutions have nonunique f_i values.

In view of such relaxed existence conditions, we may conclude that the hardly dominated boundary is by no means a rare problem feature, especially for MOPs having many objectives. However, this feature is scarcely seen in the existing multiobjective optimization test problems. This is because almost all existing multiobjective test problems [7], [15], [16], [18], [19], [42]–[47] have at least one of the following two characteristics: 1) the regularly oriented PF shape and 2) the single distance function. The test problem with the regularly oriented PF shape is in violation of the first existence condition, while the test

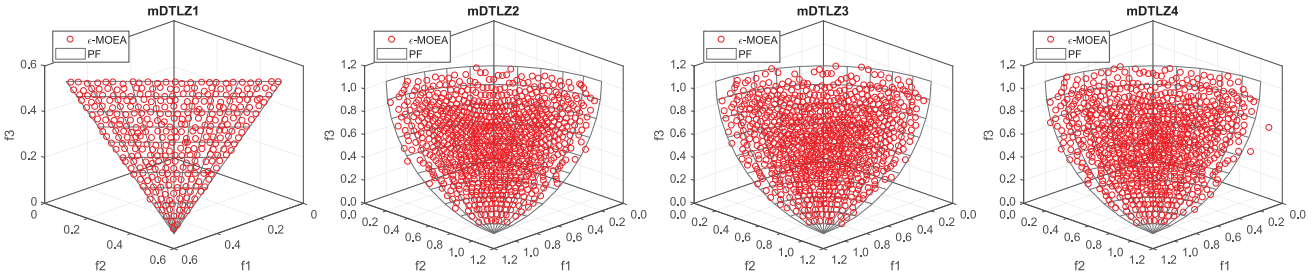

Fig. 14. Plots of the final solutions with the median Δ_2-metric values found by ϵ-MOEA in 30 runs on the three-objective mDTLZ1–mDTLZ4.

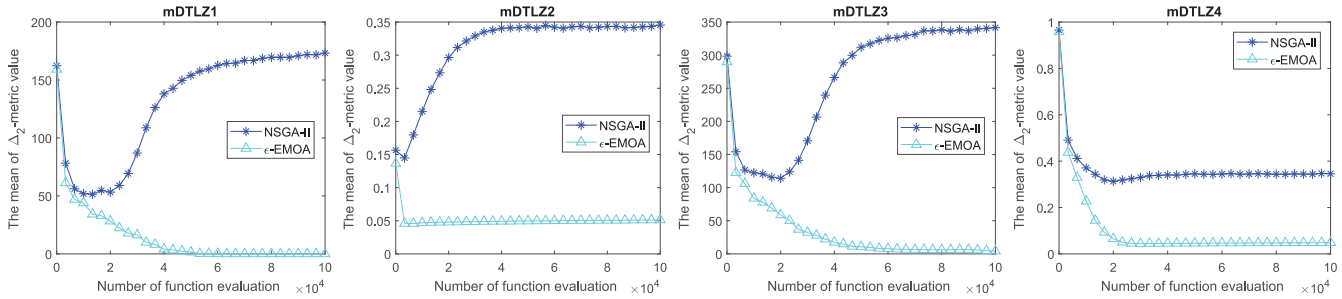

Fig. 15. Evolution of the mean Δ_2-metric values of NSGA-II and ϵ-MOEA on the three-objective mDTLZ1–mDTLZ4.

problem whose all objective functions use the same distance function violates the second existence condition. It is interesting to note that these two characteristics are precisely the two ones that have recently been regarded as lacking in generality [7].

VI. Coping Strategies

As discussed previously, the hardly dominated boundary is a common problem feature, and it can cause Pareto dominance-based MOEAs and Tchebycheff-decomposition-based MOEAs difficulty in approximating the PF. In this section, we point out and validate some possible improvement strategies for both dominance-based MOEAs and decomposition-based MOEAs to overcome the challenges caused by the hardly dominated boundary.

A. Relaxation Forms of Pareto Dominance

Considering that the dominance resistance property of the solutions on the hardly dominated boundaries arises from the strict criterion of Pareto dominance, the use of the relaxation forms of Pareto dominance (e.g., α-dominance [41] and ϵ-dominance [48]) in dominance-based MOEAs should be a possible coping strategy [49], [50]. To validate this, we operate ϵ-MOEA [51] on the mDTLZ1–mDTLZ4 problems and compare its performance to that of NSGA-II.

ϵ-MOEA is a steady-state MOEA that uses ϵ-dominance criterion to update the archive population. The concept of ϵ-dominance can be defined as follows [48], [52].

Definition 7: Let $\epsilon = (\epsilon_1, \ldots, \epsilon_m)^{\mathsf{T}}$ and $\epsilon_i > 0$ for $i = 1, \ldots, m$, a solution $\mathbf{x}^1$ is said to *ϵ-dominate* another solution $\mathbf{x}^2$, if $f_j(\mathbf{x}^1) - \epsilon_j \leq f_j(\mathbf{x}^2)$ for all $j \in \{1, \ldots, m\}$, and $f_k(\mathbf{x}^1) - \epsilon_k < f_k(\mathbf{x}^2)$ for at least one $k \in \{1, \ldots, m\}$.

In our experiments, ϵ_i is set to be 0.02 for $i = 1, \ldots, m$, and other common parameters are set to be the same as in Section IV. Fig. 14 plots the final population obtained by ϵ-MOEA that has the median Δ_2-metric value in the 30 runs on each three-objective mDTLZ problem. It is evident that ϵ-MOEA can find a good approximation for each test MOP's PF. The undesirable solutions on the hardly dominated boundaries are significantly reduced in each approximate solution set, and almost all the attained solutions are close to the PF. Fig. 15 shows the evolution of the average Δ_2-metric values achieved by NSGA-II and ϵ-MOEA with the number of function evaluations. Obviously, ϵ-MOEA is much more effective and efficient than NSGA-II in reducing the Δ_2-metric values on all these four test problems.

From these results, we may conclude that the utilization of relaxation forms of Pareto dominance is useful for dominance-based MOEAs in coping with MOPs characterized by the hardly dominated boundary.

B. Generalized Decomposition

The generalized decomposition method [53], [54] is a modified version of the Tchebycheff decomposition method, and it defines the scalar optimization subproblem as follows:

$$\begin{aligned} \text{minimize} \quad & g\left(\mathbf{x}|\mathbf{w}, \mathbf{z}^*\right) = \max_{1\leq i\leq m} \left\{ w_i \left(|f_i(x) - \left(z_i^* - \delta\right)| \right.\right. \\ & \left.\left. + \rho \sum_{j=1}^{m} |f_j(x) - \left(z_j^* - \delta\right)| \right) \right\} \\ \text{subject to} \quad & \mathbf{x} \in \Omega \end{aligned} \tag{16}$$

where the definitions of $\mathbf{w}$ and $\mathbf{z}^*$ are the same as in (2). δ and ρ are two small scalars.

As discussed in [53] and [54], subproblems achieved by the generalized decomposition method can avoid being optimal on the weakly Pareto optimal solutions. With this theory, we infer that using the generalized decomposition

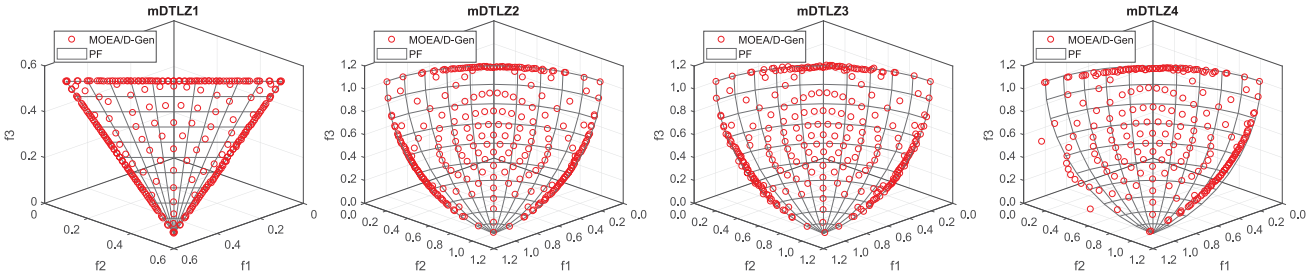

Fig. 16. Plots of the final solutions with the median Δ_2-metric values found by ϵ-MOEA in 30 runs on the three-objective mDTLZ1–mDTLZ4.

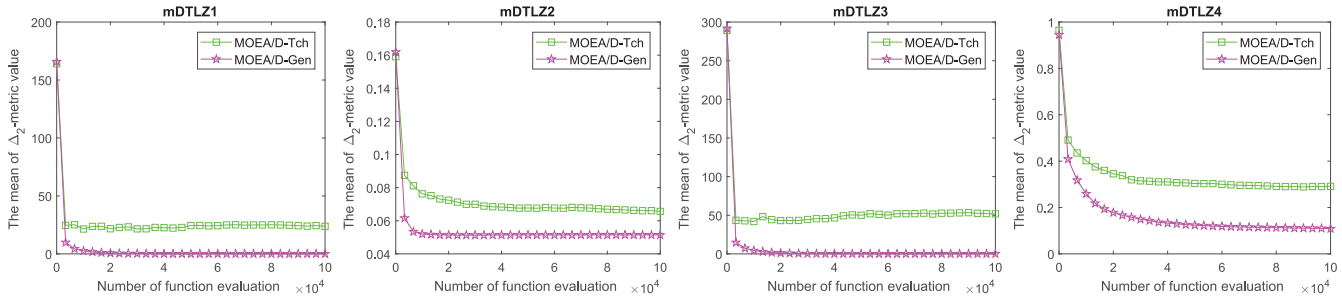

Fig. 17. Evolution of the mean Δ_2-metric values of MOEA/D-Tch and MOEA/D-Gen on the three-objective mDTLZ1–mDTLZ4.

method instead of the Tchebycheff decomposition method in the decomposition-based MOEA can prevent the algorithm from yielding undesirable solutions on the hardly dominated boundaries.

To confirm this idea, we operate a new algorithm named MOEA/D-Gen on the mDTLZ1–mDTLZ4 problems. MOEA/D-Gen is realized by replacing the Tchebycheff decomposition method in MOEA/D-Tch with the generalized decomposition method. In MOEA/D-Gen, δ and ρ are set to be 0.01, and the rest of the parameters remain the same as MOEA/D-Tch.

Fig. 16 presents the obtained solutions with the median Δ_2-metric values in 30 runs of MOEA/D-Gen on the three-objective mDTLZ1–mDTLZ4, respectively. It is clear that MOEA/D-Gen can get rid of the undesirable solutions lie on the hardly dominated boundaries. For each MOP, almost all the solutions yielded by MOEA/D-Gen are close to the PF. Furthermore, Fig. 17 provides the evolution of the mean Δ_2-metric values achieved by MOEA/D-Tch and MOEA/D-Gen versus the number of function evaluations on each MOP. It also indicates that MOEA/D-Gen outperforms MOEA/D-Tch in getting better Δ_2-metric values on all four test problems.

These results lead us to the conclusion that using the generalized decomposition method for the construction of subproblems is an efficient way for decomposition-based MOEAs to address the challenges posed by the hardly dominated boundary.

C. Estimation of Hypervolume Contributions

When dealing with the mDTLZ problem, due to the existence of many DRSs, the environmental selection of SMS-EMOA is mainly based on the solutions' HV contributions. However, the calculation of HV is very time-consuming, especially for many-objective problems (the runtime complexity is exponential in the number of objectives). An intuitive way to ease this computational burden is to use the estimation algorithm to approximate the HV contributions. Monte Carlo simulation is one of the most commonly used HV estimation methods [55].

In the first variant of SMS-EMOA, SMS-EMOA-E1, the Monte Carlo simulation (i.e., $\hat{I}_h^1$ in [55]) is employed to replace the original exact calculation of the HV contribution. However, our studies indicate that the HV contributions of many DRSs are tiny and the estimation method (i.e., $\hat{I}_h^1$) tends to approximate them as zero. As a result, the algorithm's environmental selection will be less effective since the worst solution cannot be identified. To overcome this shortcoming, another variant of SMS-EMOA (denoted as SMS-EMOA-E2) is subsequently developed. In SMS-EMOA-E2, the solutions can be further distinguished via the overall HVs (i.e., $\hat{I}_h^{|A|}$ in [55]) once their HV contributions are estimated to be zero.

SMS-EMOA-E1 and SMS-EMOA-E2 are carried out on the three-objective mDTLZ1–mDTLZ4. The solutions obtained by two algorithms with the median Δ_2-metric values in 30 runs are plotted in Fig. 21 in the supplementary material. Moreover, the evolution of the mean Δ_2-metric values achieved by SMS-EMOA, SMS-EMOA-E1, and SMS-EMOA-E2 is shown in Fig. 22 in the supplementary material. From these results, it can be concluded that SMS-EMOA-E1 fails to approximate the PFs of mDTLZ1 and mDTLZ3. The two test problems have large hardly dominated boundaries, and thereby contain numerous DRSs in the feasible regions. As mentioned earlier, the environmental selection of SMS-EMOA-E1 becomes inefficient when faced with a large number of DRSs. The solutions obtained by SMS-EMOA-E2 are mostly located on the PF of each problem. However, these solutions are not as well-distributed as the solutions yielded by SMS-EMOA. Although the two variants are not as good as SMS-EMOA in approximation quality, they are superior to SMS-EMOA in terms of computational effort, especially when dealing with many-objective problems.

VII. Discussions

A. Other Challenges Arising From the Hardly Dominated Boundary

As discussed earlier, the solutions on the hardly dominated boundary are easily treated as nondominated solutions by MOEAs, albeit they are far away from the PF. For a nondominated solution set, if it contains a large number of solutions far away from the PF, it is considered to be low-quality. Since the nondominated solution set is often used in many aspects of the evolutionary process, a low-quality one may introduce various difficulties for MOEAs. For example, it may lead to inaccurate estimations of the nadir point and the PF range [25], [45], [56], [57]. Moreover, it is also likely to pose hindrances in the normalization of objective vectors [23], [58], [59], the dynamic design of weight vectors [60]–[62], the estimation of density distribution [63]–[65], and so on. Therefore, it is crucial to eliminate the inferior solutions (far away from the PF) before utilizing the nondominated solution set for other purposes.

B. Further Improvements of the Coping Algorithms

As can be seen from Fig. 16, although MOEA/D-Gen can get rid of the hindrances induced by the hardly dominated boundary, it still cannot produce a good approximation to each problem's PF. It still suffers from the mismatch between the distribution of its subproblems and the PF shape of the mDTLZ problem [7]. The approximate solutions achieved by the majority of subproblems lie on the boundaries of the PF. A better distributed approximate solution set can be yielded by employing an external archive or adaptive weight/direction vectors in the decomposition-based MOEA [47], [66].

Furthermore, it can be found from Fig. 14 that ϵ-MOEA cannot well approximate the boundary parts of each problem's PF. This deficiency can be remedied by adding other diversity maintenance strategies to the algorithm. In addition, the approximate sets with better distributions can be achieved by SMS-EMOA if the reference point is appropriately set in its HV calculation [67]. Meanwhile, the accuracy of the HV approximation algorithm needs to be improved so that the differences between solutions having small HV contributions can be distinguished.

C. Generality of the PS and PF Shapes

Although the PF shapes used in mDTLZ1–mDTLZ4 can avoid being over-friendly to some MOEAs, their generality is still unlikely to model all real-world problems [68]. Moreover, the PS shapes of mDTLZ1–mDTLZ4 are still linear, which is not conducive to reflect the real difficulties of the test problems. For an MOP with a linear PS, once a Pareto optimal solution is found, other Pareto optimal solutions can be easily obtained by searching along the PS.

Using more complicated PS and PF in mDTLZ1–mDTLZ4 can make them more general. A simple way to achieve this is to use (17) instead of (6) to define the objective functions, and use (18) to replace the component $x_i - 0.5$ or $x_i^{100} - 0.5$ in $g_k(\mathbf{x}_{II})$ of each mDTLZ problem

$$\text{minimize} \quad f_k(\mathbf{x}) = 2k(h_k(\mathbf{x}_I))^{\alpha}(1 + g_k(\mathbf{x}_{II})) \tag{17}$$

$$2(x_i)^{\beta} - 1 - \prod_{j=1}^{m-1} \sin\left(3\pi x_j + \frac{i\pi}{n}\right) \tag{18}$$

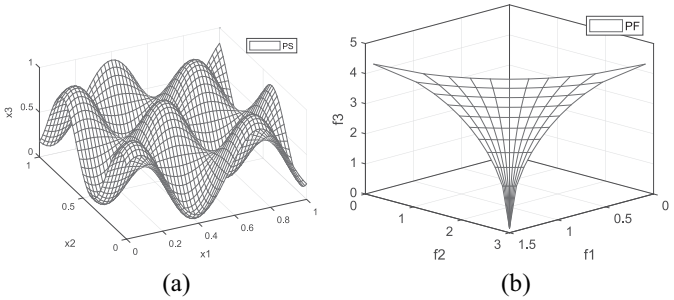

Fig. 18. Complicated (a) PS and (b) PF generated for mDTLZ1 with $m = 3$, $n = 10$, $\alpha = 0.5$, and $\beta = 1$.

where $k \in \{1, \ldots, m\}$, $i \in \{m, \ldots, n\}$ and $\alpha, \beta > 0$ are two parameters. Fig. 18 shows the PS and PF generated for mDTLZ1 using $m = 3$, $n = 10$, $\alpha = 0.5$, and $\beta = 1$.

In this paper, our primary purpose is to illustrate the existence of the hardly dominated boundary and explain how it hinders the approximation of certain MOEAs. The use of simple PS and PF shapes in mDTLZ problems is to facilitate analysis and explanation. Test problems with various PS and PF shapes will be developed and discussed in our future work.

VIII. Conclusion

In this paper, our study initiated with the DTLZ1–DTLZ4 test problems. First, we have proposed the modified variants (denoted as mDTLZ1–mDTLZ4) of the DTLZ1–DTLZ4 problems to enable them to get rid of two special characteristics: 1) the regularly oriented PF shape and 2) the single distance function. Then, three representative algorithms NSGA-II (dominance-based MOEA), MOEA/D-Tch (decomposition-based MOEA), and SMS-EMOA (indicator-based MOEA) have been tested and compared on mDTLZ1–mDTLZ4. Experimental results have shown that the performance of NSGA-II and MOEA/D-Tch deteriorates to some extent.

Through analysis, we have found that there exist the hardly dominated boundaries in each mDTLZ problem's feasible region. The solutions on the hardly dominated boundaries are easily misidentified as the Pareto optimal solutions by Pareto dominance-based MOEAs and Tchebycheff-decomposition-based MOEAs, thus impeding their approximation to the problem's PF. Further, we have revealed the conditions for the existence of the hardly dominated boundary and pointed out that it should be an often encountered MOP feature.

In addition, we have indicated and verified some possible strategies for dominance-based MOEAs and decomposition-based MOEAs in coping with MOPs featured by the hardly dominated boundary. More specifically, the challenges posed by the hardly dominated boundary can be overcome by using the relaxation forms of Pareto dominance in dominance-based MOEAs as well as using the generalized decomposition method in decomposition-based MOEAs.

Acknowledgment

The authors would like to thank Prof. Q. Zhang for his help.

References

[1] J. Branke, K. Deb, K. Miettinen, and R. Slowiński, Eds. *Multiobjective Optimization: Interactive and Evolutionary Approaches*, vol. 5252. Berlin, Germany: Springer, 2008.

[2] Y. Collette and P. Siarry, *Multiobjective Optimization: Principles and Case Studies*. Berlin, Germany: Springer, 2013.

[3] A. Mukhopadhyay, U. Maulik, S. Bandyopadhyay, and C. A. C. Coello, "A survey of multiobjective evolutionary algorithms for data mining: Part I," *IEEE Trans. Evol. Comput.*, vol. 18, no. 1, pp. 4–19, Feb. 2014.

[4] N. Al Moubayed, A. Petrovski, and J. McCall, "D^2MOPSO: Multi-objective particle swarm optimizer based on decomposition and dominance," in *Evolutionary Computation in Combinatorial Optimization*. Berlin, Germany: Springer, 2012, pp. 75–86.

[5] S. Jiang and S. Yang, "Evolutionary dynamic multiobjective optimization: Benchmarks and algorithm comparisons," *IEEE Trans. Cybern.*, vol. 47, no. 1, pp. 198–211, Jan. 2017.

[6] M. Jamil and X.-S. Yang, "A literature survey of benchmark functions for global optimisation problems," *Int. J. Math. Model. Numer. Optim.*, vol. 4, no. 2, pp. 150–194, 2013.

[7] H. Ishibuchi, Y. Setoguchi, H. Masuda, and Y. Nojima, "Performance of decomposition-based many-objective algorithms strongly depends on Pareto front shapes," *IEEE Trans. Evol. Comput.*, vol. 21, no. 2, pp. 169–190, Apr. 2017.

[8] R. Cheng, Y. Jin, M. Olhofer, and B. Sendhoff, "Test problems for large-scale multiobjective and many-objective optimization," *IEEE Trans. Cybern.*, vol. 47, no. 12, pp. 4108–4121, Dec. 2017.

[9] H.-L. Liu, L. Chen, Q. Zhang, and K. Deb, "Adaptively allocating search effort in challenging many-objective optimization problems," *IEEE Trans. Evol. Comput.*, vol. 22, no. 3, pp. 433–448, Jun. 2018.

[10] H. Wang, Y. Jin, and J. Doherty, "A generic test suite for evolutionary multi-fidelity optimization," *IEEE Trans. Evol. Comput.*, doi: 10.1109/TEVC.2017.2758360.

[11] S. B. Gee, K. C. Tan, and H. A. Abbass, "A benchmark test suite for dynamic evolutionary multiobjective optimization," *IEEE Trans. Cybern.*, vol. 47, no. 2, pp. 461–472, Feb. 2017.

[12] M. Li, C. Grosan, S. Yang, X. Liu, and X. Yao, "Multiline distance minimization: A visualized many-objective test problem suite," *IEEE Trans. Evol. Comput.*, vol. 22, no. 1, pp. 61–78, Feb. 2018.

[13] R. Cheng *et al.*, "A benchmark test suite for evolutionary many-objective optimization," *Complex Intell. Syst.*, vol. 3, no. 1, pp. 67–81, 2017.

[14] Z. Fan *et al.*, "Difficulty adjustable and scalable constrained multi-objective test problem toolkit," *arXiv preprint arXiv:1612.07603*, 2016.

[15] H.-L. Liu, L. Chen, K. Deb, and E. D. Goodman, "Investigating the effect of imbalance between convergence and diversity in evolutionary multiobjective algorithms," *IEEE Trans. Evol. Comput.*, vol. 21, no. 3, pp. 408–425, Jun. 2017.

[16] H. Li, Q. Zhang, and J. Deng, "Biased multiobjective optimization and decomposition algorithm," *IEEE Trans. Cybern.*, vol. 47, no. 1, pp. 52–66, Jan. 2017.

[17] K. Deb, "Multi-objective genetic algorithms: Problem difficulties and construction of test problems," *Evol. Comput.*, vol. 7, no. 3, pp. 205–230, Sep. 1999.

[18] S. Huband, P. Hingston, L. Barone, and L. While, "A review of multiobjective test problems and a scalable test problem toolkit," *IEEE Trans. Evol. Comput.*, vol. 10, no. 5, pp. 477–506, Oct. 2006.

[19] K. Deb, L. Thiele, M. Laumanns, and E. Zitzler, "Scalable test problems for evolutionary multiobjective optimization," in *Evolutionary Multiobjective Optimization. Theoretical Advances and Applications*. London, U.K.: Springer, pp. 105–145, 2005.

[20] K. Deb and D. Saxena, "Searching for Pareto-optimal solutions through dimensionality reduction for certain large-dimensional multi-objective optimization problems," in *Proc. IEEE Congr. Evol. Comput. (CEC)*, 2006, pp. 3352–3360.

[21] D. K. Saxena, J. A. Duro, A. Tiwari, K. Deb, and Q. Zhang, "Objective reduction in many-objective optimization: Linear and nonlinear algorithms," *IEEE Trans. Evol. Comput.*, vol. 17, no. 1, pp. 77–99, Feb. 2013.

[22] H. Ishibuchi, H. Masuda, and Y. Nojima, "Pareto fronts of many-objective degenerate test problems," *IEEE Trans. Evol. Comput.*, vol. 20, no. 5, pp. 807–813, Oct. 2016.

[23] K. Deb and H. Jain, "An evolutionary many-objective optimization algorithm using reference-point-based nondominated sorting approach, part I: Solving problems with box constraints," *IEEE Trans. Evol. Comput.*, vol. 18, no. 4, pp. 577–601, Aug. 2014.

[24] M. Asafuddoula, T. Ray, and R. Sarker, "A decomposition-based evolutionary algorithm for many objective optimization," *IEEE Trans. Evol. Comput.*, vol. 19, no. 3, pp. 445–460, Jun. 2015.

[25] K. Li, K. Deb, Q. Zhang, and S. Kwong, "An evolutionary many-objective optimization algorithm based on dominance and decomposition," *IEEE Trans. Evol. Comput.*, vol. 19, no. 5, pp. 694–716, Oct. 2015.

[26] Y. Yuan, H. Xu, B. Wang, B. Zhang, and X. Yao, "Balancing convergence and diversity in decomposition-based many-objective optimizers," *IEEE Trans. Evol. Comput.*, vol. 20, no. 2, pp. 180–198, Apr. 2016.

[27] Y. Yuan, H. Xu, B. Wang, and X. Yao, "A new dominance relation-based evolutionary algorithm for many-objective optimization," *IEEE Trans. Evol. Comput.*, vol. 20, no. 1, pp. 16–37, Feb. 2016.

[28] H. Ishibuchi, K. Doi, and Y. Nojima, "Reference point specification in MOEA/D for multi-objective and many-objective problems," in *Proc. IEEE Int. Conf. Syst. Man Cybern. (SMC)*, Budapest, Hungary, 2016, pp. 4015–4020.

[29] H. Seada and K. Deb, "A unified evolutionary optimization procedure for single, multiple, and many objectives," *IEEE Trans. Evol. Comput.*, vol. 20, no. 3, pp. 358–369, Jun. 2016.

[30] Q. Zhang and H. Li, "MOEA/D: A multiobjective evolutionary algorithm based on decomposition," *IEEE Trans. Evol. Comput.*, vol. 11, no. 6, pp. 712–731, Dec. 2007.

[31] X. Ma, Q. Zhang, G. Tian, J. Yang, and Z. Zhu, "On Tchebycheff decomposition approaches for multiobjective evolutionary optimization," *IEEE Trans. Evol. Comput.*, vol. 22, no. 2, pp. 226–244, Apr. 2018.

[32] R. Wang, J. Xiong, H. Ishibuchi, G. Wu, and T. Zhang, "On the effect of reference point in MOEA/D for multi-objective optimization," *Appl. Soft Comput.*, vol. 58, pp. 25–34, Sep. 2017.

[33] D. Brockhoff and E. Zitzler, "Objective reduction in evolutionary multiobjective optimization: Theory and applications," *Evol. Comput.*, vol. 17, no. 2, pp. 135–166, 2009.

[34] H. Masuda, Y. Nojima, and H. Ishibuchi, "Common properties of scalable multiobjective problems and a new framework of test problems," in *Proc. IEEE Congr. Evol. Comput. (CEC)*, Vancouver, BC, Canada, 2016, pp. 3011–3018.

[35] K. Deb, A. Pratap, S. Agarwal, and T. Meyarivan, "A fast and elitist multiobjective genetic algorithm: NSGA-II," *IEEE Trans. Evol. Comput.*, vol. 6, no. 2, pp. 182–197, Apr. 2002.

[36] N. Beume, B. Naujoks, and M. Emmerich, "SMS-EMOA: Multiobjective selection based on dominated hypervolume," *Eur. J. Oper. Res.*, vol. 181, no. 3, pp. 1653–1669, 2007.

[37] O. Schutze, X. Esquivel, A. Lara, and C. A. C. Coello, "Using the averaged Hausdorff distance as a performance measure in evolutionary multiobjective optimization," *IEEE Trans. Evol. Comput.*, vol. 16, no. 4, pp. 504–522, Aug. 2012.

[38] E. Zitzler and L. Thiele, "Multiobjective evolutionary algorithms: A comparative case study and the strength Pareto approach," *IEEE Trans. Evol. Comput.*, vol. 3, no. 4, pp. 257–271, Nov. 1999.

[39] H. Kita, Y. Yabumoto, N. Mori, and Y. Nishikawa, "Multi-objective optimization by means of the thermodynamical genetic algorithm," in *Proc. Int. Conf. Parallel Problem Solving from Nature (PPSN)*, Berlin, Germany, 1996, pp. 504–512.

[40] D. Hadka and P. Reed, "Borg: An auto-adaptive many-objective evolutionary computing framework," *Evol. Comput.*, vol. 21, no. 2, pp. 231–259, May 2013.

[41] K. Ikeda, H. Kita, and S. Kobayashi, "Failure of Pareto-based MOEAs: Does non-dominated really mean near to optimal?" in *Proc. IEEE Congr. Evol. Comput. (CEC)*, vol. 2. Seoul, South Korea, 2001, pp. 957–962.

[42] E. Zitzler, K. Deb, and L. Thiele, "Comparison of multiobjective evolutionary algorithms: Empirical results," *Evol. Comput.*, vol. 8, no. 2, pp. 173–195, Jun. 2000.

[43] H. Li and Q. Zhang, "Multiobjective optimization problems with complicated Pareto sets, MOEA/D and NSGA-II," *IEEE Trans. Evol. Comput.*, vol. 13, no. 2, pp. 284–302, Apr. 2009.

[44] Q. Zhang *et al.*, "Multiobjective optimization test instances for the CEC 2009 special session and competition," School Comput. Sci. Electron. Eng., Univ. Essex, Colchester, U.K., and School Elect. Electron. Eng., Nanyang Technol. Univ., Singapore, Rep. CES-487, 2008.

[45] S. Jiang and S. Yang, "An improved multiobjective optimization evolutionary algorithm based on decomposition for complex Pareto fronts," *IEEE Trans. Cybern.*, vol. 46, no. 2, pp. 421–437, Feb. 2016.

[46] H.-L. Liu, F. Gu, and Q. Zhang, "Decomposition of a multiobjective optimization problem into a number of simple multiobjective subproblems," *IEEE Trans. Evol. Comput.*, vol. 18, no. 3, pp. 450–455, Jun. 2014.

[47] F. Gu, H.-L. Liu, and K. C. Tan, "A multiobjective evolutionary algorithm using dynamic weight design method," *Int. J. Innov. Comput. Inf. Control*, vol. 8, no. 5(B), pp. 3677–3688, 2012.

[48] M. Laumanns, L. Thiele, K. Deb, and E. Zitzler, "Combining convergence and diversity in evolutionary multiobjective optimization," *Evol. Comput.*, vol. 10, no. 3, pp. 263–282, Sep. 2002.

[49] M. Li, L. Liu, and D. Lin, "A fast steady-state ε-dominance multiobjective evolutionary algorithm," *Comput. Optim. Appl.*, vol. 48, no. 1, pp. 109–138, 2011.
[50] Y. Tian, H. Wang, X. Zhang, and Y. Jin, "Effectiveness and efficiency of non-dominated sorting for evolutionary multi-and many-objective optimization," *Complex Intell. Syst.*, vol. 4, no. 3, pp. 247–263, 2017.
[51] K. Deb, M. Mohan, and S. Mishra, "Evaluating the ϵ-domination based multi-objective evolutionary algorithm for a quick computation of Pareto-optimal solutions," *Evol. Comput.*, vol. 13, no. 4, pp. 501–525, 2005.
[52] A. G. Hernández-Díaz, L. V. Santana-Quintero, C. A. C. Coello, and J. Molina, "Pareto-adaptive ε-dominance," *Evol. Comput.*, vol. 15, no. 4, pp. 493–517, 2007.
[53] K. Miettinen, *Nonlinear Multiobjective Optimization*. Boston, MA, USA: Kluwer Acad., 1999.
[54] I. Giagkiozis, R. C. Purshouse, and P. J. Fleming, "Generalized decomposition," in *Proc. Int. Conf. Evol. Multi Criterion Optim. (EMO)*, vol. 7811. Sheffield, U.K., 2013, pp. 428–442.
[55] J. Bader and E. Zitzler, "HypE: An algorithm for fast hypervolume-based many-objective optimization," *Evol. Comput.*, vol. 19, no. 1, pp. 45–76, 2011.
[56] K. Deb, K. Miettinen, and S. Chaudhuri, "Toward an estimation of nadir objective vector using a hybrid of evolutionary and local search approaches," *IEEE Trans. Evol. Comput.*, vol. 14, no. 6, pp. 821–841, Dec. 2010.
[57] H. Sato, "Inverted PBI in MOEA/D and its impact on the search performance on multi and many-objective optimization," in *Proc. 16th Annu. Genet. Evol. Comput. Conf. (GECCO)*, Vancouver, BC, Canada, 2014, pp. 645–652.
[58] K. Li, Q. Zhang, S. Kwong, M. Li, and R. Wang, "Stable matching-based selection in evolutionary multiobjective optimization," *IEEE Trans. Evol. Comput.*, vol. 18, no. 6, pp. 909–923, Dec. 2014.
[59] R. Cheng, Y. Jin, M. Olhofer, and B. Sendhoff, "A reference vector guided evolutionary algorithm for many-objective optimization," *IEEE Trans. Evol. Comput.*, vol. 20, no. 5, pp. 773–791, Oct. 2016.
[60] Y. Qi *et al.*, "MOEA/D with adaptive weight adjustment," *Evol. Comput.*, vol. 22, no. 2, pp. 231–264, 2014.
[61] S. Jiang, Z. Cai, J. Zhang, and Y.-S. Ong, "Multiobjective optimization by decomposition with Pareto-adaptive weight vectors," in *Proc. Int. Conf. Nat. Comput. (ICNC)*, vol. 3. Shanghai, China: IEEE, 2011, pp. 1260–1264.
[62] F. Gu and Y.-M. Cheung, "Self-organizing map-based weight design for decomposition-based many-objective evolutionary algorithm," *IEEE Trans. Evol. Comput.*, vol. 22, no. 2, pp. 211–225, Apr. 2018.
[63] Q. Zhang, A. Zhou, and Y. Jin, "RM-MEDA: A regularity model-based multiobjective estimation of distribution algorithm," *IEEE Trans. Evol. Comput.*, vol. 12, no. 1, pp. 41–63, Feb. 2008.
[64] V. A. Shim, K. C. Tan, and C. Y. Cheong, "A hybrid estimation of distribution algorithm with decomposition for solving the multiobjective multiple traveling salesman problem," *IEEE Trans. Syst., Man, Cybern. C, Appl. Rev.*, vol. 42, no. 5, pp. 682–691, Sep. 2012.
[65] M. Li, S. Yang, and X. Liu, "Shift-based density estimation for Pareto-based algorithms in many-objective optimization," *IEEE Trans. Evol. Comput.*, vol. 18, no. 3, pp. 348–365, Jun. 2014.
[66] X. Cai, Y. Li, Z. Fan, and Q. Zhang, "An external archive guided multiobjective evolutionary algorithm based on decomposition for combinatorial optimization," *IEEE Trans. Evol. Comput.*, vol. 19, no. 4, pp. 508–523, Aug. 2015.
[67] H. Ishibuchi, R. Imada, Y. Setoguchi, and Y. Nojima, "Reference point specification in hypervolume calculation for fair comparison and efficient search," in *Proc. 19th Annu. Genet. Evol. Comput. Conf. (GECCO)*, Berlin, Germany, 2017, pp. 585–592.
[68] A. Trivedi, D. Srinivasan, K. Pal, and T. Reindl, "A MOEA/D with non-uniform weight vector distribution strategy for solving the unit commitment problem in uncertain environment," in *Proc. Aust. Conf. Artif. Life Comput. Intell.*, Geelong, VIC, Australia, 2017, pp. 378–390.

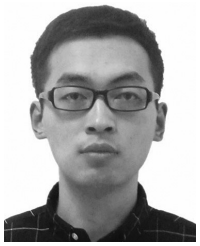

Zhenkun Wang received the Ph.D. degree in circuits and systems from Xidian University, Xi'an, China, in 2016.

He is currently a Post-Doctoral Research Fellow with the School of Computer Science and Engineering, Nanyang Technological University, Singapore. His current research interests include multiobjective optimization, evolutionary computation, test problem construction, and some machine learning techniques.

Yew-Soon Ong (M'99–SM'12–F'17) received the Ph.D. degree in artificial intelligence in complex design from the Computational Engineering and Design Center, University of Southampton, Southampton, U.K., in 2003.

He is a Professor and the Chair of the School of Computer Science and Engineering, Nanyang Technological University (NTU), Singapore, where he is also the Director of the Data Science and Artificial Intelligence Research Center and the Principal Investigator of the Data Analytics and Complex Systems Programme with the Rolls-Royce@NTU Corporate Lab, Singapore. His current research interests include computational intelligence spans across memetic computing, complex design optimization, and big data analytics.

Dr. Ong is the Founding Editor-in-Chief of the IEEE TRANSACTIONS ON EMERGING TOPICS IN COMPUTATIONAL INTELLIGENCE, the Founding Technical Editor-in-Chief of *Memetic Computing*, and an Associate Editor of the IEEE TRANSACTIONS ON EVOLUTIONARY COMPUTATION, the IEEE TRANSACTIONS ON NEURAL NETWORKS & LEARNING SYSTEMS, the IEEE TRANSACTIONS ON CYBERNETICS, and the IEEE TRANSACTIONS ON BIG DATA.

Hisao Ishibuchi (M'93–SM'10–F'14) received the B.S. and M.S. degrees in precision mechanics from Kyoto University, Kyoto, Japan, in 1985 and 1987, respectively, and the Ph.D. degree in computer science from Osaka Prefecture University, Sakai, Japan, in 1992.

He was with Osaka Prefecture University from 1987 to 2017. Since 2017, he has been the Chair Professor with the Southern University of Science and Technology, Shenzhen, China. His current research interests include fuzzy rule-based classifiers, evolutionary multi- and many-objective optimization, memetic algorithms, and evolutionary games.

Dr. Ishibuchi was the IEEE Computational Intelligence Society (CIS) Vice-President for Technical Activities from 2010 to 2013. He is an AdCom Member of the IEEE CIS from 2014 to 2019, and the Editor-in-Chief of the *IEEE Computational Intelligence Magazine* from 2014 to 2019.